

Available online at www.sciencedirect.com

ScienceDirect

www.journals.elsevier.com/journal-of-environmental-sciencesJOURNAL OF
ENVIRONMENTAL
SCIENCESwww.jesc.ac.cn

Absorption and recovery of *n*-hexane in aqueous solutions of fluorocarbon surfactants

Xiao Xiao^{1,2}, Bo Yan^{1,*}, Jiamo Fu¹, Xianming Xiao¹

1. State Key Laboratory of Organic Geochemistry and Guangdong Key Laboratory of Environmental Protection and Resources Utilization, Guangzhou Institute of Geochemistry, Chinese Academy of Sciences, Guangzhou 510640, China. E-mail: squarexiao@gig.ac.cn

2. University of Chinese Academy of Sciences, Beijing 100049, China

ARTICLE INFO

Article history:

Received 3 January 2015

Revised 22 February 2015

Accepted 12 March 2015

Available online 26 June 2015

Keywords:

Fluorocarbon surfactant

n-Hexane

Absorption

Recovery

Regeneration

ABSTRACT

n-Hexane is widely used in industrial production as an organic solvent. As an industrial exhaust gas, the contribution of *n*-hexane to air pollution and damage to human health are attracting increasing attention. In the present study, aqueous solutions of two fluorocarbon surfactants (FSN100 and FSO100) were investigated for their properties of solubilization and dynamic absorption of *n*-hexane, as well as their capacity for regeneration and *n*-hexane recovery by thermal distillation. The results show that the two fluorocarbon surfactants enhance dissolution and absorption of *n*-hexane, and their effectiveness is closely related to their concentrations in solution. For low concentration solutions (0.01%–0.30%), the partition coefficient decreases dramatically and the saturation capacity increases significantly with increasing concentration, but the changes for both are more modest when the concentration is over 0.30%. The FSO100 solution presents a smaller partition coefficient and a greater saturation capacity than the FSN100 solution at the same concentration, indicating a stronger solubilization for *n*-hexane. Thermal distillation is a feasible method to recover *n*-hexane from these absorption solutions, and to regenerate them. With 90 sec heating at 80–85°C, the recovery of *n*-hexane ranges between 81% and 85%, and the regenerated absorption solution maintains its original performance during reuse. This study provides basic information on two fluorocarbon surfactants for application in the treatment of industrial *n*-hexane waste gases.

© 2015 The Research Center for Eco-Environmental Sciences, Chinese Academy of Sciences.

Published by Elsevier B.V.

Introduction

n-Hexane is widely used as an organic solvent in several industries around the world, such as cleaning, printing, food processing, vegetable oil extraction, petroleum processing and plastics manufacturing (US EPA, 2007; Zamir et al., 2012). In China, it is applied even more extensively. For example, there are 534 enterprises using *n*-hexane in the Baoan District of Shenzhen City alone (Yang et al., 2011).

Because *n*-hexane has high volatility and high lipid solubility, its cumulative influence on human health has attracted increasing attention (CCOHS, Canadian Centre for Occupational Health and Safety, 1985; Card, 1998; ATSDR, 1999; Chen and Wu, 2004; Hu and Yu, 2006; Wu et al., 2013). *n*-Hexane mainly damages the nervous system, and causes poisoning (Yang et al., 2007) and cancer promotion (CCOHS, 1985), thus *n*-hexane pollution of the atmospheric environment cannot be ignored (Hernández et al., 2010; Yang et al., 2010). In China, *n*-hexane poisoning has occurred frequently

* Corresponding author. E-mail: yanbo2007@gig.ac.cn (Bo Yan).

(He et al., 2000; Kuang et al., 2001; Jia et al., 2005; Wu et al., 2006; Huang et al., 2012), and it has become the main occupational disease in some areas (Wang et al., 2014).

Similar to other hydrophobic VOCs (volatile organic compounds), *n*-hexane removal methods include incineration and catalytic combustion (Khan and Ghoshal, 2000; Zou et al., 2006; Li et al., 2009; Xi et al., 2012; Xu and Li, 2012; He et al., 2014), adsorption (Wu et al., 2001; Das et al., 2004; de Yuso et al., 2013; Sun et al., 2014), biodegradation (Kennes et al., 2009; Hassan and Sorial, 2007, 2010; Estrada et al., 2013), and a combination of some technologies such as biodegradation plus photocatalytic degradation (Saucedo-Lucero et al., 2014). The absorption technique is usually used in a two-phase bioreactor, and its purpose is to solubilize hydrophobic VOCs and improve the efficiency of biological treatment (Davison and Daugulis, 2003; Daugulis and Boudreau, 2003; Zhu et al., 2004; Arriaga and Revah, 2005; Muñoz et al., 2006; Li et al., 2007; Dumont et al., 2010; Eibes et al., 2010; Hassan and Sorial, 2010; Arca-Ramos et al., 2012; Edwards et al., 1991; Wang et al., 2013). However, a separate application of *n*-hexane waste gas absorption treatment has not been reported, and only limited data on the solubilization of *n*-hexane is available, and this is related to silicone oil (Muñoz et al., 2006) and some hydrocarbon surfactants (Hassan and Sorial, 2007, 2010; Wang et al., 2013).

The absorption method, characterized by simplicity and safety, low operational cost, and recyclable resources (Heymes et al., 2006a; Blach et al., 2008), has obvious advantages over other techniques for the treatment of high concentrations of VOCs. The key is the choice of absorbent with a large saturation absorption capacity to the targeted VOC or VOCs, a high removal efficiency, and capable of being renewed through a simple regeneration process (Heymes et al., 2006b). As representative special surfactants, fluorocarbon surfactants, as compared with hydrocarbon surfactants, have lower CMC (critical micelle concentration), stronger ability to reduce interfacial tension, and higher chemical and thermal stability (Kissa, 1994; Kovalchuk et al., 2014), and are therefore more suitable for absorption treatment of *n*-hexane and other hydrophobic VOCs. However, there is no report on the use of fluorocarbon surfactants in the solubilization of *n*-hexane.

In the present study, two commercial fluorocarbon surfactants (Zonyl FSO100 and Zonyl FSN100) with excellent surface activity (Szymczyk, 2011, 2013) were selected to investigate their performance in solubilization and dynamical absorption of *n*-hexane, and to examine the feasibility of both recovery and regeneration of the absorbent solution by thermal distillation. The purpose of this study is to provide basic information that will be useful for the application of the two fluorocarbon surfactants in the treatment of *n*-hexane-loaded waste gases.

1. Materials and methods

1.1. Materials

The two fluorocarbon surfactants Zonyl FSN-100 (FSN-100) and Zonyl FSO-100 (FSO-100) were purchased from Du Pont Company (USA), with a purity >99%. They are ethoxylated nonionic fluorocarbon surfactants, having respectively an

average of 14 (from 1 to 26) and 10 (from 1 to 16) polyoxyethylene units and 6 (from 1 to 9) and 5 (from 1 to 7) CF₂ groups (Szymczyk, 2013; Szymczyk et al., 2014). Both FSN-100 and FSO-100 have very low CMC values, 6.88×10^{-5} and 9.37×10^{-5} mol/L respectively (Szymczyk, 2013), equivalent to 0.05–0.06 g/L (calculated on the basis of their average molecular weight). *n*-Hexane used in the experiment was analytical reagent, and water was double distilled deionized water.

1.2. Determination of partition coefficient

The partition coefficient (*H*) of an absorbent solution can be deduced by a variety of methods (Gossett, 1987; Peng and Wan, 1997; Dumont et al., 2010). The phase ratio variation method (Peng and Wan, 1997) was used in the present study since the ratio of the gas phase concentrations is simply the ratio of the GC peak area without real quantification. The computational formula is expressed as below:

$$\frac{1}{A_p} = \frac{R_F}{H} C_L + \frac{R_F}{C_L} \times \frac{V_G}{V_L} \quad (1)$$

where, *C_L* (mol/L) is the concentration of *n*-hexane in the liquid phase; *V_L* (L) is the liquid phase volume in the headspace bottle when gas–liquid equilibrium is reached; *V_G* (L) is the gas phase volume in the headspace when gas–liquid equilibrium is reached; *R_F* (dimensionless) is the response factor of the gas chromatograph; *A_p* (dimensionless) is the gas chromatograph peak area of the gas phase; and *H* (dimensionless) is the partition coefficient.

According to this formula, a linear relation exists between $1/A_p$ and V_G/V_L , with a slope *S* ($S = R_F/C_L$) and an intercept *I* ($I = R_F/H \times C_L$). Thus, the partition coefficient (*H*) is the ratio of the slope to intercept (Peng and Wan, 1998), or

$$H = \frac{S}{I} \quad (2)$$

Experimental details are as follows. For each fluorocarbon surfactant, 100 mL aqueous solutions with different concentrations (0.01%, 0.05%, 0.1%, 0.3%, 0.5% and 1%) were prepared with 20 μL of liquid *n*-hexane added to each solution. Thus, 6 sets of solutions with different surfactant concentrations, but the same *n*-hexane concentration, were prepared for each surfactant. They were left to stand at 25°C for 1 hr (*n*-hexane was completely dissolved in the solution), and then 2, 5, 10, 15 and 20 mL samples from each 100 mL solution were transferred respectively to a series of 40 mL headspace vials. The vials were vibrated for 2 hr, allowed to stand for 0.5 hr, and then 10 μL gas from the head space of each vial was extracted by a sampling needle to measure the gas phase *n*-hexane concentration using a gas chromatograph. The *n*-hexane peak area was used to represent its concentration in the gas phase. A plot of the reciprocal of the peak area against the ratio of the gas phase volume to the liquid phase volume was made for a solution with a specific surfactant concentration, with the data showing a linear correlation. The ratio of the line slope to its intercept is the partition coefficient of the solution. For comparison with literature values, the Henry's law constant of *n*-hexane for the deionized water was determined using the same method.

The gas chromatograph was a Shimadzu GC-2010 (Japan) with a DB-wax column (30 m × 0.25 mm × 0.5 μm). The main operating conditions were: vaporizing chamber temperature 200°C, FID detector (APC-2010, Shimadzu, Japan) temperature 250°C, high purity nitrogen carrier gas, and injected sample amounts of 10 μL.

1.3. Dynamic absorption

The principle of the experimental device is shown in Fig. 1. A tank of compressed dry air (the ratio of nitrogen to oxygen being the same as for air) (1) provides an air flow with a pressure of 10⁵ Pa. The air flux was split into two paths, which were controlled by two rotary flowmeters (2). One pathway of the air was through a vessel (4: vessel 1) with some amounts of liquid *n*-hexane, and the passed air contained some amounts of *n*-hexane vapor. The gas stream was mixed with another path of clean air in another vessel (6: vessel 2) where the *n*-hexane-bearing gas was diluted to a desirable *n*-hexane concentration to form a simulated exhaust gas. The simulated exhaust gas then entered into a gas dispersing device (7) located at the bottom of a long column (8: vessel 3) filled with an absorption solution. As a result, the incoming gas was effectively dispersed to form small bubbles passing through the absorption solution. The tail gas was finally emitted from a small opening (10) at the top of the absorption vessel. During the experiment, the temperatures of the liquid *n*-hexane and absorption solution were controlled respectively by two thermostatic baths (5). The VOC background value, caused possibly by the absorption solution itself, was measured as the vessel (3) was closed, and the inlet gas *n*-hexane concentration was measured as the vessel (9) was opened. The *n*-hexane concentration in the gas flux and the inlet air

flux rate were controlled by adjusting the two rotary flowmeters (2).

For a comparison with the partition coefficient measurements, absorption experiments of the aqueous solutions of the two fluorocarbon surfactants with 6 concentrations (0.01%, 0.05%, 0.1%, 0.3%, 0.5%, 1.0%) were carried out. The absorption experiment conditions were set as 25 g of absorption solution, a temperature of 25°C, and an inlet gas flow rate of 100 L/hr with a *n*-hexane concentration of 3000 mg/m³.

1.4. Measurement of *n*-hexane concentration in gas phase

The *n*-hexane concentration in the inlet and outlet gases was measured by a VOC detector (PGM-7320, RAE, USA). The principles and characteristics of the detector were described by Xiao et al. (2013). The detector measures only the total VOC concentration; however, the investigated gas in the present study contains only *n*-hexane, therefore the total VOC is in fact the *n*-hexane concentration. The detector has a high accuracy with an error ≤3% within its detection range (<10,000 mg/m³ VOC).

For each absorption experiment, the two detectors were set to record the *n*-hexane concentration of inlet and outlet gases once a minute, until both concentrations were equal, when the tested absorbent solution was accepted as having reached its saturated absorption. The instantaneous absorptivity or removal rate (A_t , %) of *n*-hexane was computed by the Eq. (3)

$$A_t = \frac{c_0 - c_t}{c_0} \times 100\% \quad (3)$$

where, c_0 (mg/m³) is the inlet gas concentration of *n*-hexane, and c_t (mg/m³) is the outlet gas concentration of *n*-hexane.

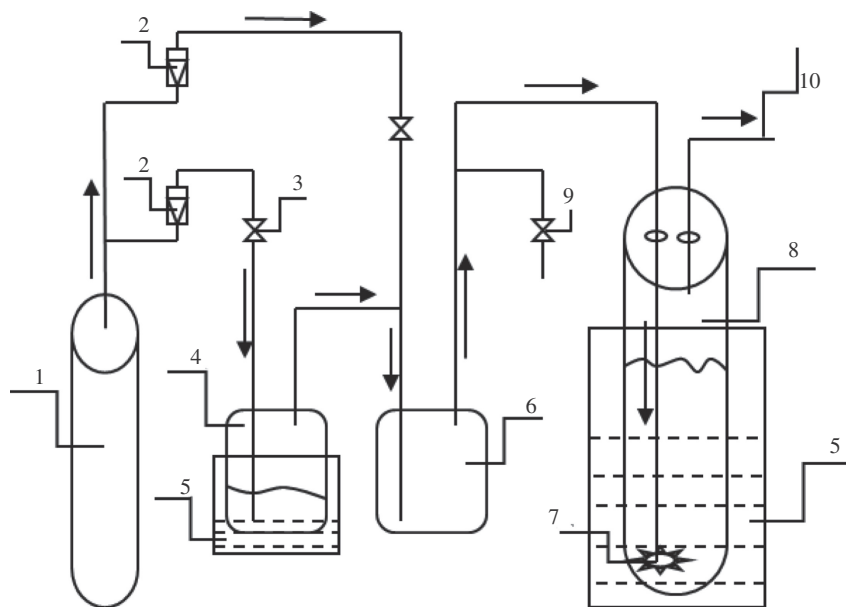


Fig. 1 – Schematic diagram showing the formation and absorption process of *n*-hexane-loaded gas. 1. Air bottle. 2. Rotary flowmeter. 3. Valve. 4. Gaseous *n*-hexane producer. 5. Thermostatic bath. 6. *n*-Hexane concentration-dilution vessel. 7. Gas dispersing device. 8. Absorption column. 9. Valve. 10. Outlet gas tube.

1.5. Calculation of *n*-hexane concentration in the liquid phase

The saturated *n*-hexane concentration (C_s , mg/g) based on the absorption curve can be calculated by Eq. (4) (Heymes et al., 2006b)

$$C_s = \frac{Q_G}{m_0} \int (c_0 - c_t) dt \quad (4)$$

where, Q_G (m^3/hr) is inlet gas flow rate; and m_0 (g) is the mass of absorption solution.

1.6. Recovery of *n*-hexane and reuse of absorption solution

In theory, such methods as solvent extraction, pervaporation, air stripping and thermal distillation can all recover *n*-hexane from an absorbent solution in different degrees, and thereby regenerate it (Heymes et al., 2006a, 2006b). Considering the low boiling point of *n*-hexane (68.7°C) and the good thermal stability of the fluorocarbon surfactants used, we chose thermal distillation for this purpose. The experiment consisted of three steps: (1) Two absorbent solutions respectively with a FSN100 and FSO100 concentration of 0.30% and their corresponding saturated *n*-hexane concentrations (based on the dynamic absorption experiment results) were prepared. (2) The influence of heating temperature and heating time on the recovery rate of *n*-hexane was investigated for the two absorbent solutions to determine the distillation conditions. The heating temperature was set from 65 to 90°C, around the boiling point of *n*-hexane. A pre-test indicated that an azeotrope was formed for the two absorbent solutions when the temperature was increased to close to the boiling point of *n*-hexane, and most of the *n*-hexane was distilled out from the absorption solution within 1–2 min. Thus, the heating duration was set from 30 to 150 sec. (3) With distillation conditions determined from the above steps, each absorption solution (with a FSN100 or FSO100 concentration of 0.30%) was reused 5 times under the conditions described above, including absorption and distillation processes, and the saturated absorption concentration and *n*-hexane recovery rate was calculated for each cycle. The *n*-hexane recovery rate (R_n , %) at n times of reuse is calculated by Eq. (5):

$$R_n = \frac{C_{nr}}{C_{ns}} \times 100\% \quad (5)$$

where, C_{ns} (mg/g) is the saturation *n*-hexane concentration of the absorption solution at n times of reuse; and C_{nr} (mg/g) is the recovered *n*-hexane concentration from the absorption solution at n times of reuse.

2. Results and discussion

2.1. Partition coefficient

According to literature values, the Henry's law constant of *n*-hexane at 20–30°C ranges from 36.75 to 42.4 (Ashworth et al., 1988; Vergara-Fernández et al., 2006; Yang et al., 2010). A similar value of 39.87 at 25°C was obtained from the present study, confirming the reliability of the method used.

Table 1 – *n*-Hexane partition coefficients (H) for the aqueous solutions of two fluorocarbon surfactants at 25°C.

Concentration (%)	H (FSN100)	H (FSO100)
0.01	11.91	9.51
0.05	11.18	8.89
0.1	10.11	7.78
0.3	4.48	3.21
0.5	3.10	2.13
1	1.32	1.09

Table 1 presents the *n*-hexane partition coefficients of the absorbent solutions. Fig. 2 highlights the relationship between the partition coefficients and concentrations. In the investigated concentration range (0.01%–1.0%), the partition coefficient of FSO100 is smaller than that of FSN100, indicating its stronger solubilization capacity. FSO100 has a similar CMC value, but a shorter ethoxy chain length as compared with FSN100 (Szymczyk, 2013; Szymczyk et al., 2014). According to a study carried out by Yeom et al. (1996), a greater ethoxy chain length for ethoxylated nonionic surfactants will decrease the solubilization effect on hydrophobic organic compounds, a possible reason for the partition coefficient difference between the two fluorocarbon surfactants.

The partition coefficients of both FSN100 and FSO100 solutions decrease with increasing concentration, but the slope of the curve decreases in the higher concentration range, with a clear inflection point at about 0.30% (Fig. 2). A similar trend was reported by Yang et al. (2010) for the four hydrocarbon surfactants of sodium dodecyl sulfate (SDS), cetyltrimethylammonium bromide (CTAB), tert-octylphenoxypolyethoxyethanol (Triton X-100), and polyoxyethylene (20) sorbitan monooleate (Tween 80) in solubilizing *n*-hexane, however the inflection point concentrations vary widely for the four hydrocarbon surfactants, with a value of 5 g/L for SDS, 3 g/L for CTAB, 1.5 g/L for Triton X-100 and >4.5 g/L for Tween 80. They believe that this trend could be caused by a change in micelle structure as the surfactant concentration increases. As the surfactant concentration increases to a certain amount (0.5% for the two fluorocarbon surfactants), excessive micelles occur and the solubilization ability could

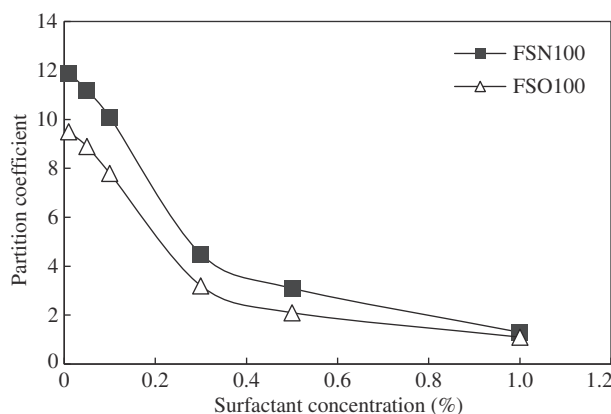


Fig. 2 – Changes in *n*-hexane partition coefficients with concentration for the fluorocarbon surfactants.

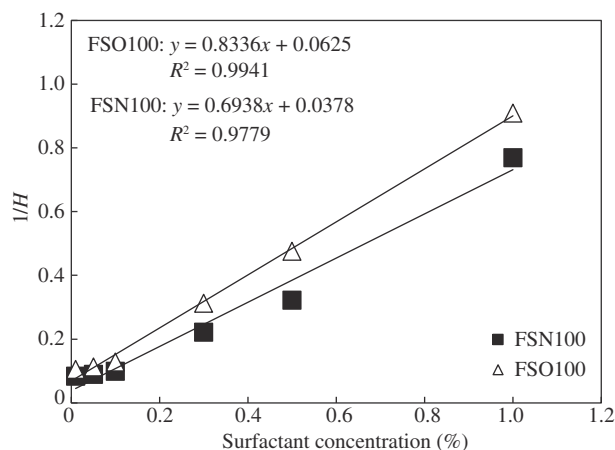


Fig. 3 – Plot showing the relationship between the reciprocal of partition coefficients (1/H) and the concentrations of the studied FSN100 and FSO100 solutions.

be affected by their interaction, which would restrain the general solubilization performance to some extent.

According to the data presented by Yang et al. (2010), the *n*-hexane partition coefficient of Triton X-100 is the smallest among the above hydrocarbon surfactants. As compared with the present results, both FSN100 and FSO100, have an even smaller partition coefficient at the same concentration, indicating a greater solubilization. For instance, at a concentration of 0.1%, the partition coefficients of Triton X-100, FSN100 and FSO100 are 16.3, 10.11 and 7.78, respectively. The CMC value of Triton X-100 is 0.112 g/L (Yang et al., 2010), while those of FSN100 and FSO100 are about 0.05–0.06 g/L (see Section 1.1). This means many more micelles can be formed from FSN100 and the FSO100 at the same concentration, which should be the main reason for their larger solubilization capacity compared to the hydrocarbon surfactants.

Matsuoka et al. (2014) investigated the solubilization of naphthalene and octafluoronaphthalene in some ionic fluorocarbon surfactants. They attributed the quite low solubilization to their small aggregates (micelles) composed of nonflexible fluorocarbon chains, which might not be good at solubilizing fluorocarbon and hydrocarbon compounds owing to their own

close-packed aggregate structures. Both FSN-100 and FSO-100 are ethoxylated nonionic fluorocarbon surfactants. Non-ionic surfactants are generally applied to make oil-in-water emulsions (Myers, 1992), and exhibit stronger solubilization of hydrophobic VOCs, as compared with anionic or cationic surfactants with a similar length hydrophobic chain (Kile and Chiou, 1989). According to the data reported from Szymczyk (2013), the average size of their aggregates is close to that of a sphere having a radius ranging from 15.70 to 32.30 Å when the concentration is greater than their CMC values, thus with quite enough space to trap *n*-hexane (4.9 Å molecular size), which would be a reason of their obvious solubilization toward *n*-hexane in the present study. This implies that the solubilization capacity of fluorocarbon surfactants, similar to hydrocarbon surfactants (Liu et al., 2010), is also strongly related to their structures as well as the properties of solubilizates, although there are currently quite limited data available (Matsuoka et al., 2014).

A linear relation was observed between the reciprocal of partition coefficients and the concentrations of the studied FSN100 and FSO100 solutions, with a correlation coefficient of 0.98 and 0.99, respectively (Fig. 3), similar to the results for the four hydrocarbon surfactants investigated by Yang et al. (2010). Therefore, the *n*-hexane partition coefficient of a fluorocarbon surfactant solution can be also deduced from its concentration.

2.2. Absorption efficiency

Fig. 4 presents the *n*-hexane absorption curves of aqueous solutions of FSO100 and FSN100 with different concentrations. An increase of the absorbent concentration can improve the absorptivity and increase the saturation concentration. However, when the absorbent concentration reaches a certain level (about 0.3%), the saturation concentration increase becomes very slow. Taking FSO100 as an example, as its concentration increases from 0.01% to 0.3%, the initial absorptivity and saturation concentration of *n*-hexane increase from 79% to 91% and from 1.5 mg/g to 2.9 mg/g respectively, however, when its concentration increases further from 0.3% to 1%, the initial absorptivity and saturation concentration only increase from 91% to 93% and from 2.9 mg/g to 3.2 mg/g, respectively (Figs. 4 and 5). Comparing FSO-100 and FSN-100 solutions, the

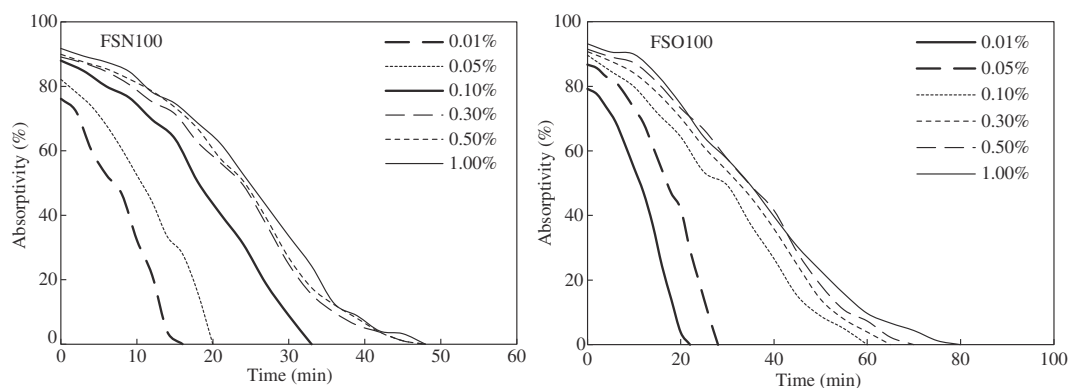


Fig. 4 – Absorption curves of the aqueous solutions of FSO100 and FSN100 with different concentrations.

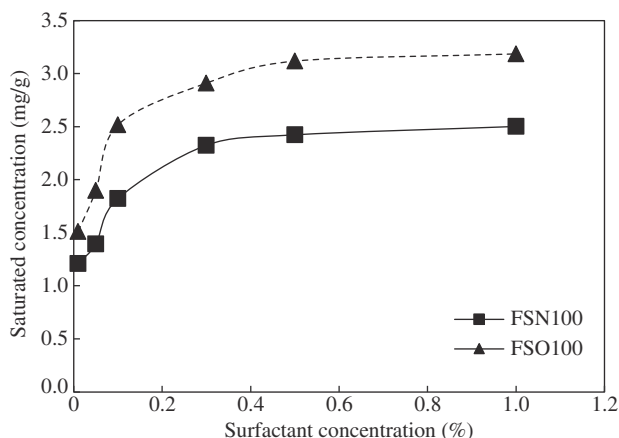


Fig. 5 – Relationship between absorbent (FSO100 and FSN100) concentration in solution and saturation concentration of *n*-hexane.

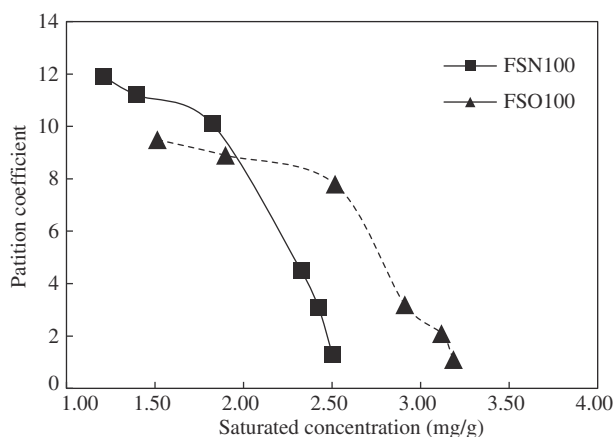


Fig. 6 – Relationship between the saturation concentration and partition coefficient for the FSO100 and FSN100 solutions.

former has a greater saturation concentration (Fig. 5), consistent with the solubilization capacity indicated by the partition coefficients (Fig. 2).

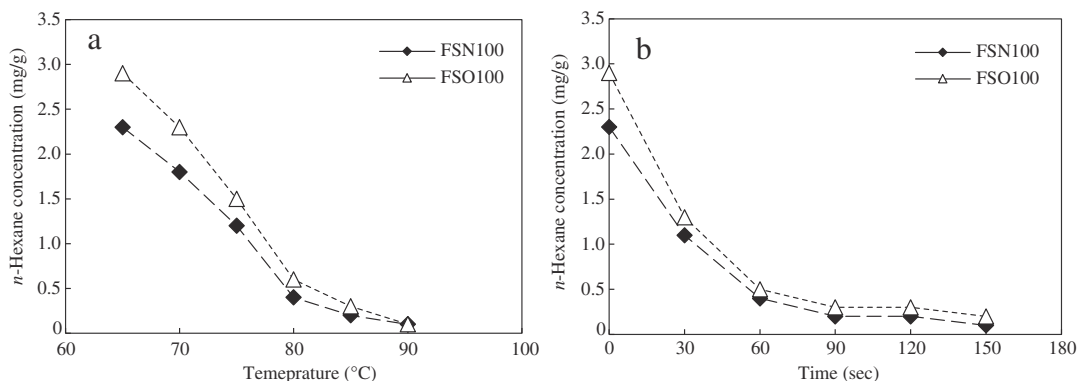


Fig. 7 – Changes in *n*-hexane concentration in the absorbent solution with increasing temperature (a: 90 sec heating time for each temperature point) and time (b: at the temperature of 85°C).

As the partition coefficient of the absorbent solutions decreases, the absorption saturation concentration increases, but this is not a linear relationship (Fig. 6). For low concentration solutions (0.01%–0.1%), a small decrease of the partition coefficient corresponds to a large increase in the saturation concentration. However, with a further decrease of the partition coefficient (0.1%–1.0% of the absorbent concentration), the increase of the saturated absorption concentration becomes slower. This shows that the dynamic absorption process of *n*-hexane cannot be fully explained by the partition coefficient. As the *n*-hexane concentration in the absorption solution is increased to a certain degree, there is no corresponding increase in the saturated absorption concentration, even if the absorption solution has a very low partition coefficient. This is mainly because the gas–liquid mass transfer process is not only related to the characteristics of the absorption solution, but also is influenced significantly by operating conditions as well as the absorption device (Yeom et al., 1996). In spite of this, the partition coefficient is the main factor controlling the concentration of saturated absorption for solutions with the same absorbent.

2.3. Recovery of *n*-hexane and regeneration of absorbent solution

The distillation experiments were carried out on FSN100 and FSO100 solutions with an absorbent concentration of 0.3%, and *n*-hexane concentrations of 2.3 mg/g and 2.9 mg/g respectively, which are equal to their absorption saturation concentrations. When the heating temperature was increased to 80–85°C, most of the *n*-hexane was distilled out from the solution in a very short period of time (60–90 sec; Fig. 7a). With an extension of time of distillation, the amount of distilled *n*-hexane was not significantly increased (Fig. 7b). Thus, the temperature to recover *n*-hexane from the absorbent solution was set at 80–85°C with a distillation duration of 90 sec.

Five repeated reuses of the FSN100 and FSO100 absorbent solutions gave essentially the same absorption curves (Fig. 8), indicating an identical absorption performance. The absorption efficiency of the initial solution was slightly better than that of the reused solution (Fig. 9). This is because the distillation cannot completely recover the *n*-hexane from the absorbent solution, with a residual of 0.2–0.3 mg/g, which

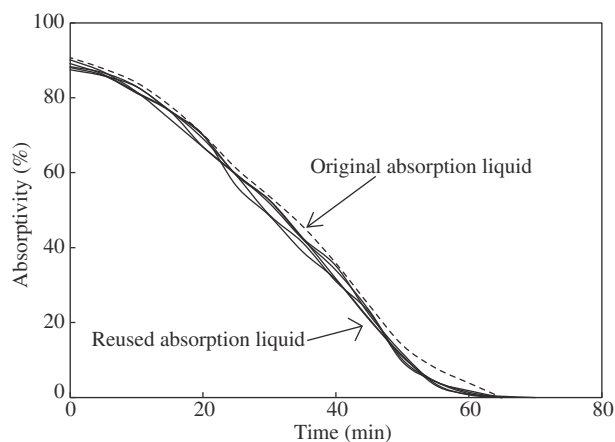


Fig. 8 – Absorption curves of FSO-100 absorbent solution during several reuses in comparison with the initial solution.

slightly reduces the absorption efficiency during the reuse. The *n*-hexane recovery rate during the five reuse cycles is similar, as high as 81%–85% (Fig. 10). Therefore, the thermal distillation ($\leq 85^{\circ}\text{C}$) does not destroy the chemical structure of the fluorocarbon surfactant, showing that this is a feasible method for recovering *n*-hexane and regenerating the absorbent solution.

3. Conclusions

The following conclusions were obtained through the study on solubilization, absorption and recovery of *n*-hexane in aqueous solutions of two fluorocarbon surfactants (FSN-100, FSO-100). (1) The two fluorocarbon surfactants are very effective in the solubilization of *n*-hexane, and the partition coefficients are controlled by their concentration. For the low concentration (0.01%–0.30%) solutions, the partition coefficients decrease with the increase of absorbent concentration; however, as the concentration is increased above 0.3%, the decrease

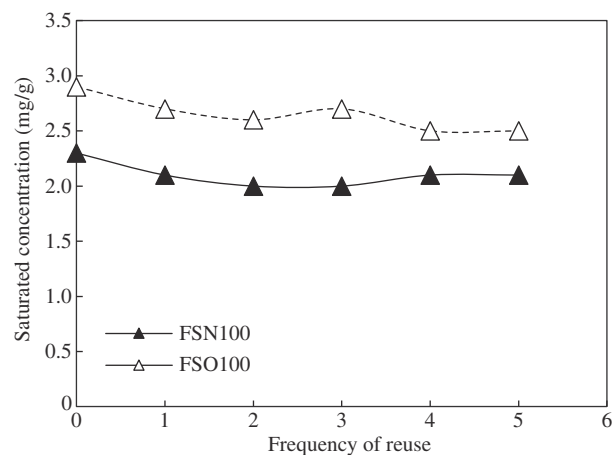


Fig. 9 – Changes of saturated absorption concentration of *n*-hexane for the FSN100 and FNO100 absorbent solutions during reuse (inlet gas concentration 3000 mg/m³).

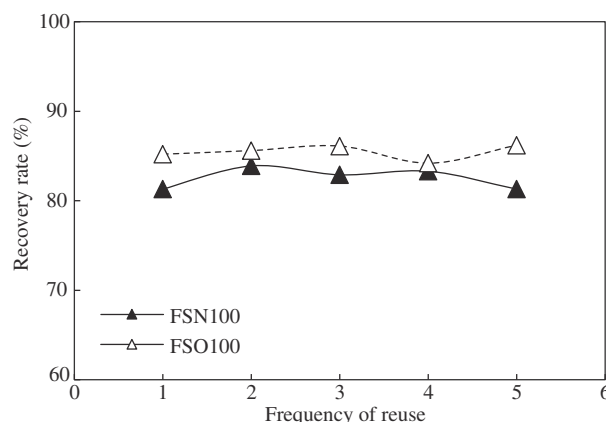


Fig. 10 – Changes of recovery rate of *n*-hexane for the FNS100 and FNO100 absorbent solutions during reuse (inlet gas concentration 3000 mg/m³).

in partition coefficient becomes much slower. (2) The absorption of *n*-hexane by the two fluorocarbon surfactants follows a similar pattern to the partition coefficient. Within the concentration range of 0.01%–0.30%, the saturation concentration increases strongly with increasing concentration, whereas the saturation concentration increases only slightly within the concentration range from 0.30% to 1.0%. (3) Compared with hydrocarbon surfactants reported in the literature, the two fluorocarbon surfactants have a stronger solubilizing capacity for *n*-hexane. Of the fluorocarbon surfactants FSO100 and FSN100, the former has the higher solubilization capacity. (4) Thermal distillation is highly efficient in recovering *n*-hexane from the absorbent solutions, and in regenerating them. Under the conditions of 80–85°C and 90 sec heating duration, the *n*-hexane recovery rate reaches 81%–85%, and the regenerated absorption solution maintains its initial absorption capacity during several reuses.

Acknowledgments

The authors are indebted to the anonymous reviewers for their insightful comments and suggestions that have significantly improved the manuscript, and to Dr. Wilkins, R.W.T. from CSIRO of Australia for improving the English language of this article. This research was supported by Guangdong Natural Science Funds for Distinguished Young Scholar (No. S2013050014122) and Guangzhou Institute of Geochemistry, Chinese Academy of Sciences (No. 2012-03) (135 project). This is contribution No. IS-2062 from GIGGAS.

REFERENCES

Arca-Ramos, A., Eibes, G., Moreira, M.T., Feijoo, G., Lema, J.M., 2012. Surfactant-assisted two phase partitioning bioreactors for laccase-catalyzed degradation of anthracene. *Process Biochem.* 47 (7), 1115–1121.
 Arriaga, A., Revah, S., 2005. Improving hexane removal by enhancing fungal development in a microbial consortium biofilter. *Biotechnol. Bioeng.* 90 (10), 7–15.

- Ashoworth, R.A., Howe, G.B., Mullins, M.E., Rogers, T.N., 1988. Air-water partitioning coefficients of organics in dilute aqueous solutions. *J. Hazard. Mater.* 18 (1), 25–36.
- ATSDR, 1999. Toxicological profile for n-hexane. US Department of Health and Human Services. Agency for Toxic Substances and Disease Registry. Public Health Service, Atlanta, GA, USA.
- Blach, P., Fourmentin, S., Landy, D., Cazier, F., Surpateanu, G., 2008. Cyclodextrins: a new efficient absorbent to treat waste gas streams. *Chemosphere* 70 (3), 374–380.
- Card, T.R., 1998. *Fundamentals: Chemistry and Characteristics of Odors and VOCs*. McGraw-Hill, New York.
- CCOHS (Canadian Centre for Occupational Health and Safety), 1985. n-Hexane. Chemical Hazard Summary. 11 Hamilton, Ontario.
- Chen, Y.H., Wu, A.S., 2004. An investigation of n-hexane occupation disease and prevention in an industrial area of China. *Occup. Health* 30 (3), 162–163.
- Das, D., Gaur, V., Verma, N., 2004. Removal of volatile organic compound by activated carbon fiber. *Carbon* 42 (14), 2949–2962.
- Daugulis, A.J., Boudreau, N.G., 2003. Removal and destruction of high concentrations of gaseous toluene in a two-phase partitioning bioreactor by *Alcaligenes xylosoxidans*. *Biotechnol. Lett.* 25 (17), 1421–1424.
- Davison, C.T., Daugulis, A.J., 2003. Addressing biofilter limitations: a two-phase partitioning bioreactor process for the treatment of benzene and toluene contaminated gas streams. *Biodegradation* 14 (6), 415–421.
- De Yuso, A.M., Izquierdo, M.T., Valenciano, R., Rubio, B., 2013. Toluene and n-hexane adsorption and recovery behavior on activated carbons derived from almond shell wastes. *Fuel Process. Technol.* 110 (1), 1–7.
- Dumont, E., Darracq, G., Couvert, A., Couriol, C., Amrane, A., Thomas, D., et al., 2010. Determination of partition coefficients of three volatile organic compounds (dimethylsulphide, dimethyldisulphide and toluene) in water/silicone oil mixtures. *Chem. Eng. J.* 162 (3), 927–934.
- Edwards, D.A., Luthy, R.G., Liu, Z., 1991. Solubilization of polycyclic aromatic hydrocarbons in micellar nonionic surfactant solutions. *Environ. Sci. Technol.* 25 (1), 127–133.
- Eibes, G., McCann, C., Pedezert, A., Moreira, M.T., Feijoo, G., Lema, J.M., 2010. Study of mass transfer and biocatalyst stability for the enzymatic degradation of anthracene in a two-phase partitioning bioreactor. *Biochem. Eng. J.* 51 (1–2), 79–85.
- Estrada, J.M., Lebrero, R., Quijano, G., Kraakman, N.J.R., Munoz, R., 2013. Strategies for odour control. In: Belgiorno, V., Naddeo, V., Zarra, T. (Eds.), *Odour Impact Assessment Handbook*. John Wiley & Sons, New Jersey, pp. 85–124.
- Gossett, J.M., 1987. Measurement of Henry's law constants for C1 and C2 chlorinated hydrocarbons. *Environ. Sci. Technol.* 21 (1), 202–208.
- Hassan, A.A., Sorial, G.A., 2007. Enhancing the destruction of hydrophobic VOCs in trickle bed air biofilter. A&WMA's 100th Annual Conference & Exhibition, Pittsburg, USA, pp. 1045–1059.
- Hassan, A.A., Sorial, G.A., 2010. A comparative study for destruction of n-hexane in trickle bed air biofilter. *Chem. Eng. J.* 162 (1), 227–233.
- He, J.X., Li, L.Y., Huang, X.Q., 2000. Survey of n-hexane occupation harm in Shenzhen city. *China Occup. Med.* 27 (5), 50–51.
- He, Z.F., He, Z.R., Wang, D., Bo, Q.F., Fan, T., Jiang, Y., 2014. Mo-modified Pd/Al₂O₃ catalysts for benzene catalytic combustion. *J. Environ. Sci.* 26 (7), 1481–1487.
- Hernández, M., Quijano, G., Thalasso, F., Daugulis, A.J., Villaverde, S., Munoz, R., 2010. A comparative study of solid and liquid non-aqueous phases for biodegradation of hexane in two-phase partitioning bioreactors. *Biotechnol. Bioeng.* 106 (5), 731–740.
- Heymes, F., Manno-Demoustier, P., Charbit, F., Fanlo, J.L., Moulin, P., 2006a. Recovery of toluene from high temperature boiling absorbent by pervaporation. *J. Membr. Sci.* 284 (1), 145–154.
- Heymes, F., Manno-Demoustier, P., Charbit, F., 2006b. A new efficient absorption liquid to treat exhaust air loaded with toluene. *Chem. Eng. J.* 115 (3), 225–231.
- Hu, W., Yu, H.Z., 2006. Progress of n-hexane poisoning study Shanghai. *J. Prev. Med.* 18 (9), 473–476.
- Huang, Z.S., Zhong, X.P., Zhu, Z.L., 2012. Investigation of the present situation of n-hexane occupation harm for 108 enterprises in Guanlan area of Shenzhen City. *China Trop. Med.* 12 (7), 855–861.
- Jia, H.L., Liu, R.Y., Li, H., 2005. Four cases of chronic n-hexane poisoning. *Occup. Health* 31 (4), 272–273.
- Kennes, C., Rene, E.R., Veiga, M.C., 2009. Bioprocesses for air pollution control. *J. Chem. Technol. Biotechnol.* 84 (10), 1419–1436.
- Khan, F.I., Ghoshal, A.K., 2000. Removal of volatile organic compounds from polluted air. *J. Loss Prev. Process Ind.* 13 (6), 527–545.
- Kile, D.E., Chiou, C.T., 1989. Water solubility enhancements of DDT and trichlorobenzene by some surfactants below and above the critical micelle concentration. *Environ. Sci. Technol.* 23 (7), 832–838.
- Kissa, E., 1994. *Fluorinated Surfactants, Synthesis, Properties, Applications*. Surfactant Science Series, Marcel Dekker, Inc., New York.
- Kovalchuk, N.M., Trybala, A., Starov, V., Matar, O., Ivanova, N., 2014. Fluoro-vs hydrocarbon surfactants: why do they differ in wetting performance? *Adv. Colloid Interface Sci.* 210 (1), 65–71.
- Kuang, S.R., Huang, H.L., Liu, H.F., Chen, J.B., Kong, L.Z., Chen, B.J., 2001. A clinical analysis of 102 cases of n-hexane chronic poisoning. *Dep. Intern. Med.* 40 (5), 44–46.
- Li, W.X., Bi, Y., Yu, S.S., Ji, Z.L., Yang, L.H., Wang, X., 2007. Effect of addition of the third phase on gas-liquid mass transfer. *Chem. Indus. Eng.* 24 (6), 536–544.
- Li, W.B., Wang, J.X., Gong, H., 2009. Catalytic combustion of VOCs on non-noble metal. *Catal. Today* 148 (1–2), 81–87.
- Liu, L., Tian, S.L., Ning, P., 2010. Principle and prediction for absorption of toluene by solubilization with Tween-20-containing micelle solutions. *China Environ. Sci.* 30 (5), 615–618.
- Matsuoka, K., Yamashita, R., Ichinose, M., Kondo, M., Yoshimura, T., 2014. Solubilization of naphthalene and octafluoronaphthalene in ionic hydrocarbon and fluorocarbon surfactants. *Colloids Surf. A* 456, 83–91.
- Muñoz, R., Arriaga, S., Hernández, S., Guieysse, B., Revah, S., 2006. Enhanced hexane biodegradation in a two phase partitioning bioreactor: overcoming pollutant transport limitations. *Process Biochem.* 41 (7), 1614–1619.
- Myers, D., 1992. *Surfactant Science and Technology*. 2nd ed. Wiley-VCH, New York, pp. 240–265.
- Peng, J., Wan, A., 1997. Measurement of Henry's constants of high volatility organic compounds using a headspace autosampler. *Environ. Sci. Technol.* 31 (10), 2998–3003.
- Peng, J., Wan, A., 1998. Effect of ionic strength on Henry's constants of volatile organic compounds. *Chemosphere* 36 (13), 2731–2740.
- Saucedo-Lucero, J.O., Quijano, G., Arriaga, S., Muñoz, R., 2014. Hexane abatement and spore emission control in a fungal biofilter-photoreactor hybrid unit. *J. Hazard. Mater.* 276 (2), 287–294.
- Sun, X.J., Miao, J.P., Xiao, J., Xia, Q.B., Zhao, Z.X., 2014. Heterogeneity of adsorption sites and adsorption kinetics of n-hexane on metal-organic framework MIL-101(Cr). *Chin. J. Chem. Eng.* 22 (9), 955–960.
- Szymczyk, K., 2011. The properties of binary mixtures of ethoxylated octyl phenols with ethoxylated fluorinated

- alkanols at the water/air interface. *J. Surfactant Deterg.* 14 (3), 415–423.
- Szymczyk, K., 2013. Behaviour of the fluorocarbon surfactants in the monolayer at the water–air interface and in the bulk phase. *J. Fluor. Chem.* 150 (1), 109–116.
- Szymczyk, K., González-Martín, M.L., Bruque, J.M., Jańczuk, B., 2014. Effect of two hydrocarbon and one fluorocarbon surfactant mixtures on the surface tension and wettability of polymers. *J. Colloid Interface Sci.* 417 (1), 180–187.
- US EPA (Environmental Protection Agency), 2007. Hexane 2007 Available at: <http://www.epa.gov/ttn/atw/hlthef/hexane.html>.
- Vergara-Fernández, A., Van Haaren, B., Revah, S., 2006. Phase partition of gaseous hexane and surface hydrophobicity of *Fusarium solani* when grown in liquid and solid media with hexanol and hexane. *Biotechnol. Lett.* 28 (24), 2011–2017.
- Wang, L., Yang, C.P., Cheng, Y., Huang, J., He, H.J., Zeng, G.M., et al., 2013. Effects of surfactant and Zn(II) at various concentrations on microbial activity and ethylbenzene removal in biotricking filter. *Chemosphere* 93 (11), 2909–2913.
- Wang, L.H., Fan, Z.Y., Wang, P., Wang, L.P., Zhou, X.S., Zheng, J., 2014. Occupation disease status in Jinshan District of Shanghai city from 2000 to 2012. *Occup. Health* 30 (4), 436–438.
- Wu, J., Xie, Z., Guo, K., Claesson, O., 2001. Measurement and prediction of the adsorption of binary mixtures of organic vapors on activated carbon. *Adsorpt. Sci. Technol.* 19 (9), 737–749.
- Wu, Z.Y., Hu, J.J., Yang, J.R., Zhang, X., Wang, J., Qiu, S.L., 2006. Accident investigation of n-hexane poisoning from a shoe-made factory. *China J. Prevent. Med.* 7 (3), 217–218.
- Wu, L.K., Tian, Y.F., Zhu, Z.L., 2013. Development and evaluation of protection guide on n-hexane occupation harm. *Occup. Health Emerg. Rescue* 31 (3), 170–171.
- Xi, J.Y., Wu, J.L., Hu, H.Y., Wang, G., 2012. Application status of industrial VOCs gas treatment techniques. *China Environ. Sci.* 32 (11), 1955–1960.
- Xiao, X., Yan, B., Fu, J.M., 2013. A comparison study of toluene absorption capability by several kinds of organic solvents. *Chin. J. Environ. Eng.* 7 (3), 1072–1078.
- Xu, B.J., Li, W.B., 2012. Removal of n-hexane in exhaust gas using MnOx/TiO₂ catalytic combustion. *Environ. Prot. Chem. Ind.* 32 (4), 372–376.
- Yang, J.R., Zhang, X., Wang, J., Qian, Y.L., Wu, Z.Y., Wang, Y.H., Pang, M.T., 2007. Study on peripheral nerve damage caused by exposure to n-hexane. *China Occup. Med.* 34 (6), 462–464.
- Yang, C.P., Chen, F.Y., Luo, S.L., Xie, G.X., Zeng, G.M., Fan, C.Z., 2010. Effects of surfactants and salt on Henry's constant of n-hexane. *J. Hazard. Mater.* 175 (1–3), 187–192.
- Yang, J.P., Liu, Y.M., Wu, L.K., Zhu, Z.L., Tang, H.W., Ye, X.L., 2011. Analysis of n-hexane-used enterprises in Baoan District of Shenzhen city from 2006 to 2009. *China Occup. Med.* 38 (4), 357–358.
- Yeom, I.T., Ghosh, M.M., Cox, C.D., 1996. Kinetic aspects of surfactant solubilization of soil-bound polycyclic aromatic hydrocarbons. *Environ. Sci. Technol.* 30 (5), 1589–1595.
- Zamir, S.M., Halladj, R., Sadraei, M., Nasernejad, B., 2012. Biofiltration of gas-phase hexane and toluene mixture under intermittent loading conditions. *Process Saf. Environ. Prot.* 90 (4), 326–332.
- Zhu, X., Suidan, M.T., Pruden, A., Yang, C., Alonso, C., Kim, B.J., et al., 2004. Effect of substrate Henry's constant on biofilter performance. *J. Air Waste Manag. Assoc.* 54 (4), 409–418.
- Zou, L., Luo, Y.G., Hooper, M., Hu, E., 2006. Removal of VOCs by photocatalysis process using adsorption enhanced TiO₂-SiO₂ catalyst. *Chem. Eng. Process.* 45 (11), 959–964.